A Heading Estimation Algorithm for Wrist Device Assisted by Sequential Geomagnetic Observations

Ye Tian, Ao Peng, *Member, IEEE*, Xueting Xu, *Student Member, IEEE*, and Weicheng Zhang, *Graduate Student Member, IEEE*

***Abstract*—Pedestrian positioning with wearable devices is a significant application of attitude tracking. It tracks the attitude (with heading angle being the most important part) of the device in real time and provides positioning services for users based on the information of step length provided by Pedestrian Dead-Reckon (PDR), which is a cheap and efficient positioning method at present. However, amid a train of positioning methods, the joint estimate of tracking is given by a train of methods based on the direction of gravity and the earths magnetic field direction. Considering the measurement of gravity that the gravity accelerometer is exposed to heavy noise due to the complex movement of human body during walking with uniform swing arm posture and forward speed, this paper proposed a novel estimate method based on the Kalman filter with multi-state constraints and the usage of low-cost sensors, which fulfills the estimation with the sequential observation of magnetic field. Compared with other related work, this method proposed in this paper eliminates the dependence on gravity direction, avoiding the influence of heavy noise caused by additional linear acceleration in motion state, and reduces the influence of insufficient observation when using magnetic field observation alone. The performance of the proposed method is evaluated by real-world experimentation results.**

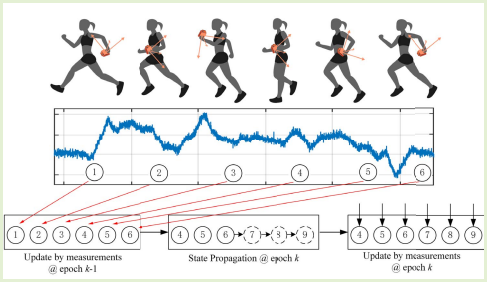

***Index Terms*—Orientation estimation, sequential geomagnetic observation, multi-state constrain, wearable device positioning.**

I. Introduction

With the development of attitude tracking research, it has been applied in diverse fields, including machine interaction [1], robotics [2], aerospace [3], navigation [4], [5], and human motion analysis [6], [7]. The tracking methods based on sensor generate the attitude angle with the integral of gyroscope, leading to a larger zero bias of the measurement with gyroscope due to the low cost of sensor. Large errors will occur in the integration process. In addition, the attitude angle calculation based on gyroscope measurement can only obtain the relative position in the sensor frame rather than the absolute position in the navigation frame.

Manuscript received May 7, 2021; revised July 18, 2021; accepted July 18, 2021. Date of publication July 21, 2021; date of current version March 14, 2022. This work was supported by the National Key Research and Development Program of China under Grant 2018YFB0505202. The associate editor coordinating the review of this article and approving it for publication was Prof. Masanori Sugimoto. *(Corresponding author: Ao Peng.)*

The authors are with the School of Informatics, Xiamen University, Xiamen 361005, China (e-mail: pa@xmu.edu.cn).

Digital Object Identifier 10.1109/JSEN.2021.3098847

Therefore, in the relevant work, the attitude is constrained by two absolute directions by the gravity measured by the accelerometer and magnetic field direction measured by the magnetometer to obtain the absolute attitude and eliminate the errors of the gyroscope. Namely, in the paper [8], [9] and [10], an optimization method based on gradient descent is proposed, which uses the direction of gravity direction and magnetic direction to estimate the attitude and integrates with gyro information with a certain weight. More specifically, Wöhle and Gebhard [9] add the Kalman filter on the basis of [8] to optimize fusion weight. Admiraal *et al.* [10] propose an optimal gradient descent algorithm to improve the operation speed and accuracy of the method in [8]. Different from optimization-based approaches, a constrained particle filter (IMeDeT) method is proposed in [11]. A scheme using extended Kalman filter (EKF) to fuse inertial navigation system (INS) and magnetometer information is proposed in [12]. In paper [13], a two-level cascade Kalman filter is proposed. All the above methods use the integrated observation of gravity direction and geomagnetic direction to ensure the full rank of the observation equation.

However, for the positioning of wearable devices under the movement scene, the sensor will generate additional linear acceleration along with the movement of human body, and the measurement of gravity will contain heavy noise. Given the observation is incomplete, the paper [14] proposes an improved complementary filtering method that only uses the information of gyroscope and accelerometer, which causes the terrible accuracy, compared with the EKF method. In [15], an improved gravity estimation method is proposed to complete the estimation of the gravity as much as possible with the accelerometer under motion state, and meanwhile the weight of gravity observation is reduced in orientation estimation. In [16], a calibration method of magnetometer is proposed, but the premise is that the acceleration sum term was restrained to be small.

Different from the above methods, in order to avoid the influence of heavy noise on gravity measurement, this paper abandons the observation on gravity, and aims at the problem of insufficient observation, the Kalman filter with multiple state constraints is used to conduct attitude estimation with the sequential observation on magnetic field. When a pedestrian is walking with uniform swing arm posture and forward speed, the proposed algorithm can provide a stable heading estimation of the walking.

II. Problem Description

A 6-axis inertial measurement unit (IMU) can provide acceleration and angular rate in body frame. But in most applications, the position and attitude need to be described in a geographic frame such as Earth-Centered Earth-Fixed (ECEF) frame or local East-North-Up (ENU) frame. The transformation of attitude from body frame to the geographic frame can be expressed by

$$s^G = C\left(q_b^G\right) s^b \tag{1}$$

where s denotes the reference direction vector respect to different frames; superscript b and G represent the body frame and geographic frame, respectively; q_G^b is the quaternion representing a rotation from geographic frame to body frame and $C\left(q_G^b\right)$ is the corresponding direction cosine matrix (DCM).

To estimate the rotation q_G^b, two reference direction is necessary. With a single reference direction, there will be an infinite number of solutions for attitude calculation. In other words, there will be an infinite number of rotation ways for a certain direction vector to rotate from the global frame to the sensor body frame. Therefore, most of the attitude and heading reference systems (AHRS) choose to use two reference directions to constrain the pose together and obtain a unique solution, such as gravity and magnetic field direction.

The acceleration observed by the on-board IMU can be written as,

$$a_m^b = C\left(q_G^b\right) g + n_a \tag{2}$$

where a_m^b is the output of accelerometer; g is the gravity vector in geographic frame; n_a is the noise induced by the accelerometer. Meanwhile, the geomagnetic field observed by the on-board magnetometer can be written as,

$$m^b = C\left(q_G^b\right) m^G + n_m \tag{3}$$

where m^b is the output of magnetometer; m^G is the geomagnetic vector in geographic frame, which may be distorted by magnetizers in the environment; n^m is the measurement noise of magnetometer. In traditional approaches [8], [9] [10], the attitude estimation uses accelerometer measurement and magnetic measurement with constraints of known gravity direction and geomagnetic direction with respect to the geographic frame as equation(4).

$$\begin{cases} a_m^b = C\left(q_G^b\right) g + n_a \\ m^b = C\left(q_G^b\right) m^G + n_m \end{cases} \tag{4}$$

Such approaches are effective for static or quasi-static objects, since the gravity vector can be treated as a constant and the measurements of the accelerometer are only decided by the attitude of the sensor. However, the gravity constraint is no longer available for moving objects such as wrist-mounted devices. Due to the periodical movement of human arms during running or walking, an unknown and time-variant linear acceleration component cannot be ignored in the measurements, which can be written as follows,

$$a_m^b = a_l^b + C\left(q_G^b\right) g + n_a \tag{5}$$

where a_l^b is the linear acceleration observed by the accelerometer in sensor body frame, which is caused by the human motion. If the measurements of accelerometer are still used, the linear acceleration should also be estimated, and it will cause the observation equation to be underdetermined because the number of observations is smaller than the number of variables. So if the gravity constraint is still used, there will be an unpredictable error obtained from the gradient descent optimization, and the result will not converge to the gravity reference direction.

However, in the scenario of motion, the measurement of magnetometer is always the geomagnetic direction, which is not affected by the motion state such as human arm movement. In the scenario we describe, the observation of the geomagnetic field can be considered reliable. Therefore, the geomagnetic measurement is used as the only constraint in the proposed approach to track the attitude. Because of the insufficient rank of underdetermined equations, the constraint of a single magnetic field observation to the attitude tracking is weak, which may easily induce cycle slip or divergence due to the observation noise.

Consider a time sequential iteration process, attitude can be calculated by gyroscope observation can be written as,

$$\begin{cases} C\left(q_G^b\right)_{k+1} = C\left(\Delta t(w_k^b + b_g + n_g)\right) C\left(q_G^b\right)_k \\ C\left(q_G^b\right)_{k+2} = C\left(\Delta t(w_{k+1}^b + b_g + n_g)\right) C\left(q_G^b\right)_{k+1} \\ \quad\vdots \\ C\left(q_G^b\right)_{k+i} = C\left(\Delta t(w_{k+i-1}^b + b_g + n_g)\right) C\left(q_G^b\right)_{k+i-1} \end{cases} \tag{6}$$

where subscript k is the epoch number, Δt is the sampling time, w_k is the instantaneous angular velocity of sensor,

b_g is the gyroscope bias and n_g is the measurement noise of gyroscope. Regard b_g as a slowly varying variable, so in a sliding time window, obtain the gyroscope iteration equations of i epochs, variables in the equations are only the initial attitude $C\left(q_G^b\right)_k$ and bias b_g. On this basis,

$$\begin{cases} m_k^b = C\left(q_G^b\right)_k m^G + n_m \\ m_{k+1}^b = C\left(q_G^b\right)_{k+1} m^G + n_m \\ \quad\vdots \\ m_{k+i}^b = C\left(q_G^b\right)_{k+i} m^G + n_m \end{cases} \tag{7}$$

proceed independent observation to the geomagnetic direction of each epoch, with the increase of observation epoch, the rank of observation equation will increase, and the observation equations will gradually become overdetermined.

As analyzed above, in this paper, multiple observations obtained sequentially are used jointly to update attitude estimates in multiple time slots, simultaneously, which is also called multi-state constrain (MSC) update. Increasing the number of independent geomagnetic observations, or the length of observation window, can reduce the uncertainty generated by the single reference direction.

III. Algorithm Description

In this section, the system model and updating mechanism based on an extended Kalman filter is described. The influence of the earth's rotation is ignored considering the accuracy of a low-cost Micro-Electro-Mechanical System (MEMS) IMU. The attitude is expressed by a rotation from the geographic frame to the sensor body frame.

A. System Model

The state vector of the proposed heading estimation algorithm consists of 3-dimensional value of local geomagnetic field and a sequence of quaternions representing rotations from ECEF frame to sensor body frame in different time, which is given by

$$X_k = \left\{ \left(m^G\right)^T, b_g, \left(q_G^{b_1}\right)^T, \ldots, \left(q_G^{b_N}\right)^T \right\}^T \tag{8}$$

where the subscript k denotes the k-th updating epoch of the proposed system, b_g is gyro bias, it is a slow time-varying variable, which is treat as invariant in a sliding window here. m^G is the 3-dimensional value of local geomagnetic field, $q_G^{b_i}$ is the quaternions from ECEF frame to body frame b_i, which is the IMU body frame defined at the moment when the i-th magnetometer measurement is obtained, N is the total number of magnetic observations used in the system, and T is matrix transpose operator. The local geomagnetic field is modeled as a constant or a slow changed variable with inaccuracy prior information.

An error state implementation is used for the state propagation, which is defined by

$$\tilde{X}_k = X_k - \bar{X}_k = \left\{ \left(\tilde{m}^G\right)^T, \tilde{b}_g, \delta q_1^T, \ldots, \delta q_N^T \right\}^T \tag{9}$$

where $\bar{X}_k$ is the prior estimation of X_k, $\tilde{m}^G$ is the estimation error of local geomagnetic field, $\tilde{b}_g$ is the error of gyro bias and δq_i is the quaternion error for the i-th body frame, which is defined by

$$q_G^{b_i} = \delta q_i \otimes \bar{q}_i \tag{10}$$

where $\bar{q}_i$ is a prior estimation of $q_G^{b_i}$, and $\otimes$ is the quaternion multiplication operator. Under small attitude error assumption, the following approximation can be used,

$$\delta q_i \approx \begin{bmatrix} [1.5]1 & \frac{1}{2}\delta\theta_i^T \end{bmatrix}^T \tag{11}$$

where $\delta\theta_i \in \mathbb{R}^{3\times 1}$ is the error of Euler angles.

The prior estimation of attitude is obtained by using the angular-rate measured from the gyroscope. The discrete propagation equation of attitude can be derived from the continuous differential equation in quaternion form, which is given by

$$\dot{q}_G^{b_i} = \frac{1}{2} q_G^{b_i} \otimes \omega_b \tag{12}$$

where $\omega_b = \begin{bmatrix} \omega_x & \omega_y & \omega_z \end{bmatrix}$ is the 3-dimensional angular-rate measured by the gyroscope. Then we can obtain the linearized continuous dynamics for the error state,

$$\begin{aligned} \dot{\tilde{X}} &= F\tilde{X} + Gn_g \\ &= \begin{pmatrix} [1.5]-1 & 0 & 0 & 0 & \omega_z & -\omega_y \\ 0 & -1 & 0 & -\omega_z & 0 & \omega_x \\ 0 & 0 & -1 & \omega_y & -\omega_x & 0 \end{pmatrix} \tilde{X} \\ &\quad - \begin{pmatrix} [1.5]1 & 0 & 0 \\ 0 & 1 & 0 \\ 0 & 0 & 1 \end{pmatrix} n_g \end{aligned} \tag{13}$$

where n_g is measurement noise of gyroscope. The discrete propagation equation of error state can be derived by solving equation (13), which is,

$$\tilde{X}_{k,k-1} = \Phi_{k,k-1}\tilde{X}_{k-1} = \exp\left[\int_{t_{k-1}}^{t_{k-1}+\Delta t} F(\tau)\, d\tau\right] \tilde{X}_{k-1} \tag{14}$$

where Δt is the sampling interval of magnetometer, and $F(\tau)$ is defined by the angular-rate at time τ. If the gyroscope is not synchronized with the magnetometer, or the sampling frequencies are not the same, interpolation for angular-rate is necessary. The matrix exponential in equation (14) is then approximated to the 3rd order Taylor series, which can be considered to be accurate enough when the sampling frequency is 50Hz,

$$\begin{aligned} \Phi_{k,k-1} &= \begin{bmatrix} \Phi_{(b_g)k,k-1} & \Phi_{(q)k,k-1} \end{bmatrix} \\ &\approx \begin{bmatrix} O_3 & I_3 \end{bmatrix} + F(t)\,\Delta t \\ &\quad + \frac{1}{2}[F(t)\,\Delta t]^2 + \frac{1}{6}[F(t)\,\Delta t]^3 \end{aligned} \tag{15}$$

For convenience of express, the 6×3 matrix $\Phi_{k,k-1}$ is divided into two 3×3 square matrices $\Phi_{(b_g)k,k-1}$ and $\Phi_{(q)k,k-1}$ by column. When a new magnetic measurement is recorded, the latest attitude error is propagated by using $\Phi_{k,k-1}$ in the current error state vector and then added to the end of the state

vector. As the new attitude error state is added, the covariance matrix of state estimation error also needs to be expanded as follows,

$$\begin{aligned} P_{q_{k,k-1}} &= \begin{bmatrix} [1.3]I_{3(N+1)\times 3(N+1)} \\ J_{k,k-1} \end{bmatrix} P_{q_{k-1}} \begin{bmatrix} [1.3]I_{3(N+1)\times 3(N+1)} \\ J_{k,k-1} \end{bmatrix}^T \\ &+ \begin{bmatrix} [1.3]O_{3(N+1)\times 3(N+1)} & O_{3(N+1)\times 6} \\ O_{6\times 3(N+1)} & Q_k \end{bmatrix} \end{aligned} \tag{16}$$

where $J_{k,k-1} = \begin{bmatrix} O_{3\times 3} & \Phi_{(b_g)k,k-1} & O_{3\times 3(N-1)} & \Phi_{(q)k,k-1} & O_{3\times 3} \end{bmatrix}$ is the propagation matrix of estimation error, and Q_k refers to the noise induced by gyroscope measurement. We have

$$Q_k = \int_{t_{k-1}}^{t_{k-1}+\Delta t} \Phi_{\tau,k-1} G Q_{k-1} G^T \Phi_{\tau,k-1}^T d\tau \tag{17}$$

The local geomagnetic field is considered as a constant during the updating interval, so the complete prior covariance of error state estimate is

$$P_{k,k-1} = \begin{bmatrix} P_{m_k} & & O \\ & P_{b_g} & \\ O & & P_{q_{k,k-1}} \end{bmatrix} \tag{18}$$

where P_{m_k} is the posterior covariance of local geomagnetic field estimate, P_{b_g} is the covariance of gyro bias.

The length of error state vector is growing by time since the latest attitude error state is added during each propagation. We set a maximum length of the error state vector. The oldest state will be deleted from the state vector when reaching the maximum length.

B. Observation Model

Considering the observation of earth magnetic field from the 3-axis magnetometer, the measurement obtained is a 3-dimensional vector with geomagnetic direction in sensor body frame. In the system described in this paper, the coordinates of inertial sensors and the magnetometer can be treated as the same. So the measured geomagnetic field is as follows,

$$m^b = C\left(q_G^b\right)\left(m^G + d_m\right) + n_m \tag{19}$$

where m^b denotes the measurement of magnetometer in body frame, m^G is the local geomagnetic field in the geography frame, d_m is local geomagnetic distortion caused by buildings or vehicles nearby, and n_m is the measurement noise of magnetometer.

Since the error state is used for system model, we choose to use the residual of observed geomagnetic field to form the observation model, which is defined by

$$\begin{aligned} \tilde{m}^b &= m^b - \hat{m}^b \\ &= C\left(q_G^b\right)\left(m^G + d_m\right) - C\left(q_G^b\right)\hat{m}^G + n_m \end{aligned} \tag{20}$$

where $\hat{m}^G$ is the posterior estimate of geomagnetic field after the latest updating. The linear approximation of equation (21) is obtained by the first order Taylor expansion as follows,

$$\tilde{m}_i^b \approx h_{q_i}\delta q_i + h_i \tilde{m}_i^G + C\left(\hat{q}_G^{b_i}\right) d_m + n_m \tag{21}$$

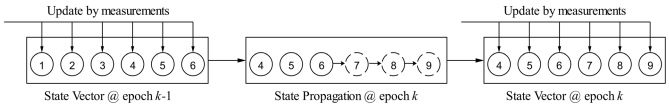

Fig. 1. Illustration of proposed attitude estimation approach.

where the subscript index i denotes the i-th measurement residual corresponding to the i-th state in the error state vector. The Jacobian matrix is defined as follows

$$h_{q_i} = \left.\frac{\partial \tilde{m}_i^b\left(\delta q_i, \tilde{m}_i^G\right)}{\partial \delta q_i}\right|_{\hat{X}_k} = \left[\, C\left(\hat{q}_G^{b_i}\right) m_i^b \,^\wedge \,\right] \tag{22}$$

where $\left[\, a \,^\wedge \,\right]$ denotes the skew-symmetric matrix of vector a, and

$$h_i = \left.\frac{\partial \tilde{m}_i^b\left(\delta q_i, \tilde{m}_i^G\right)}{\partial \tilde{m}_i^G}\right|_{\hat{X}_k} = C\left(\hat{q}_G^{b_i}\right) \tag{23}$$

For the error state vector consists of states in multiple epoch, the total measurement matrix is defined as follows,

$$H_k = \begin{bmatrix} h_i & O_{3\times 3} & h_{q_1} & O & O \\ \vdots & \vdots & O & \ddots & O \\ h_N & O_{3\times 3} & O & O & H_{q_N} \end{bmatrix} \tag{24}$$

where h_N represents the partial derivative of observation equation H respect on geomagnetic direction in ENU system of each epoch. O represents zeros matrix with size corresponding to other matrix blocks.

C. Attitude Estimation Based on Extended Kalman Filter

The attitude is estimated by an extended Kalman filter. Multiple measurements from magnetometer in time sequence are used simultaneously to update attitude estimates at different sampling time, which is so-called a multi-state constrain Kalman filter [17]. The duration of an update epoch is decided by the number of measurements used for state update, which is denoted by M. It should be noticed that M can be different to N, which is the number of states included in the error state vector.

The proposed attitude estimation approach is illustrated by Fig. 1. At the beginning of each update epoch, M oldest attitude state in the error state vector is deleted, and M new attitude state is propagated by the measurements of IMU, as detailed described in section 3.1. The attitude states added to the error state vector is synchronized with the magnetometer measurements. When M new geomagnetic field measurement is collected, the N attitude states in the error state vector, as well as the geomagnetic filed intensity, are updated simultaneously by the measurements. In this way, the repeated using of measurement is avoided, while the older states are retained in the state vector, the historic information can be taken into account during the estimation, which can improve the robustness against the temporary distortion of geomagnetic field. In additional, by controlling the maximum length of the state vector, the tradeoff between computational complexity and accuracy can be adjusted.

Algorithm 1 Attitude Estimation by MSCKF

Input: IMU measurements $\left\{a_i^b, \omega_i^b\right\}_{i=1}^M$, geomagnetic field intensity $\left\{m_i^b\right\}_{i=1}^M$

Output: quaternions from ECEF to body frame $\left\{q_G^{b_i}\right\}_{i=1}^M$

Initialize geomagnetic field intensity m^G and attitude in the form of quaternion $q_G^{b_0}$ by $\left\{a_i^b, \omega_i^b, m_i^b\right\}$ in a static scenario
for *each update epoch* **do**
  Obtain $\left\{m_i^b\right\}_{i=1}^M$ from magnetometer
  State/covariance propagation with $\left\{\omega_i^b\right\}_{i=1}^M$, refer to (14)-(18)
  Filter gain computation, refer to equation (26)
  Error state update by measurement, refer to equation (25)
  Covariance update, refer to equation (27)
  Calculate $\left\{q_G^{b_i}\right\}_{i=1}^M$ from ECEF to body frames based on the updated error state for output, refer to equation (10)
end

The EKF update process can be expressed as follows,

$$\tilde{X}_k = \tilde{X}_{k,k-1} + K_k r_k \tag{25}$$

where $r_k = \left[m_{1,k}^b - \hat{m}^b \cdots m_{M,k}^b - \hat{m}^b\right]$ is the residual vector of geomagnetic field intensity, and the filter gain is given by

$$K_k = P_{k,k-1} H_k^T \left(H_k P_{k,k-1} H_k^T + R_k\right)^{-1} \tag{26}$$

where R_k is the covariance matrix of observation noise, which is a diagonal matrix.

The posterior covariance of error state estimate is then obtained by

$$P_k = (I - K_k H_k)\, P_{k,k-1} (I - K_k H_k)^T + K_k R_k K_k^T \tag{27}$$

Considering the computational complexity of the algorithm. Matrix multiplication is the main consumption of computing in the algorithm, in an observation and update process, in equation (26), Kalman gain K can be computed in $O((3M)^3)$ operations, in equation (27), updated covariance matrix can be computed in $O((6(N+1))^3)$ operations.

The algorithm is described in Algorithm 1.

IV. Experimental Results and Analysis

Under the scenario we concerned in this paper, the purpose of our algorithm is to improve the PDR positioning accuracy of wrist device. Moreover, in the existing PDR algorithms, it has been able to realize high-precision estimation of step length, therefore, the main source of wrist device PDR positioning error is heading estimation. Based on above considerations, we integrate the proposed heading estimation algorithm and the existing step length estimation algorithm into PDR algorithm, and use the accuracy of PDR positioning result to evaluate the performance of our algorithm. Considering that we use the low-cost sensor, we pre-calibrate the gyroscope before the experiment by using map-based method [18], to eliminate gyroscope in advance.

TABLE I
Manufactory Information of Sensors Used for Experiments

Sensor Type	Manufacturer Part Number	Sampling Rate
Accelerator	BMI160	50 Hz
Gyroscope	BMI160	50 Hz
Magnetometer	AK09911	50 Hz

The performance of the proposed algorithm is evaluated by real-world experimentation results. A commercial off-the-shelf smartphone with android operation system is used to collect data from different sensors including accelerator, gyroscope, magnetometer and Global Navigation Satellite System (GNSS), which are used for post-processing. The manufactory information of the integrated sensor in the Android 8.0 smartphone is listed in Table I.

The performance of the proposed algorithm is evaluated in a standard track and field oval, compared with some traditional approaches including Madgewick Filter using gravity and magnetic field intensity and EKF using single magnetic field intensity. The smartphone is mounted on the right arm by a wristband, close to the wrist, and then the actor walked along the track line in a normal stance for nearly 2.5 laps, in totally about 7 minutes.

At the beginning of the experiment, the device kept static and steady for nearly 20 seconds. The initial estimate of earths magnetic field is derived by using the average of the measurements from magnetometer. It should be notice that the magnetic north is regarded as an approximate of geodetic north in the proposed algorithm, so there is a fixed system error in the estimate of heading angle. The initial estimate of quaternion from ECEF to sensor body frame is also obtained in the static period through a traditional Madgewick Filter.

The estimated heading angles by different algorithms in the track and field oval are shown in Fig. 2. The two straight parts of the track can be used as the ground truth reference. The positioning results from GNSS is used for mapping sensor time to the ground position. It can be seen in the figure that the Madgewick Filter cannot provide a steady estimate of heading angle during walking. For instance, during 40-60 seconds, the deviation of the estimated angle can be more than 0.6 cycle, which is about 216 degree, and also shows an obvious periodicity with frequency close to stride rate of walking. It also shows that the occurrence of cycle slip when using Madgewick Filter is more frequent than the proposed algorithm. The estimate results from EKF show a bias in comparison with the proposed algorithm, which can be found during 40-60 seconds, as well as in 220-280 seconds if the ambiguity of whole cycles induced by cycle slip is ignored. It can also be found that the estimated heading angles from EKF in the straight part of the track is not stable in 220-280 seconds. The reason is that one single magnetic measurement used in EKF is not sufficient to constrain the

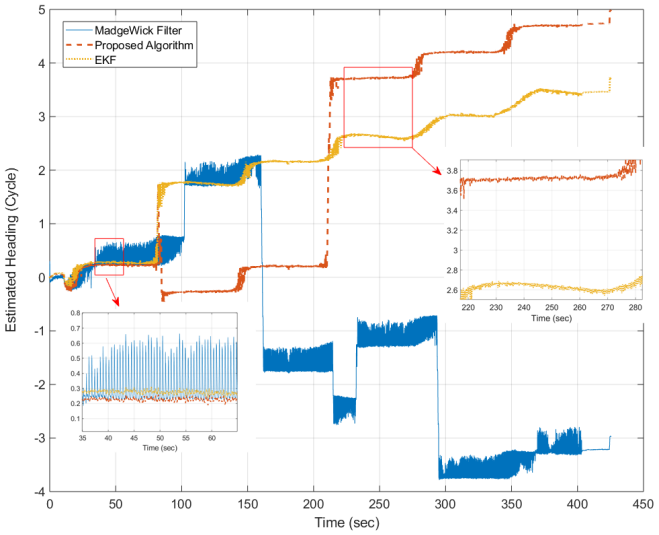

Fig. 2. Estimated heading angles by different algorithms.

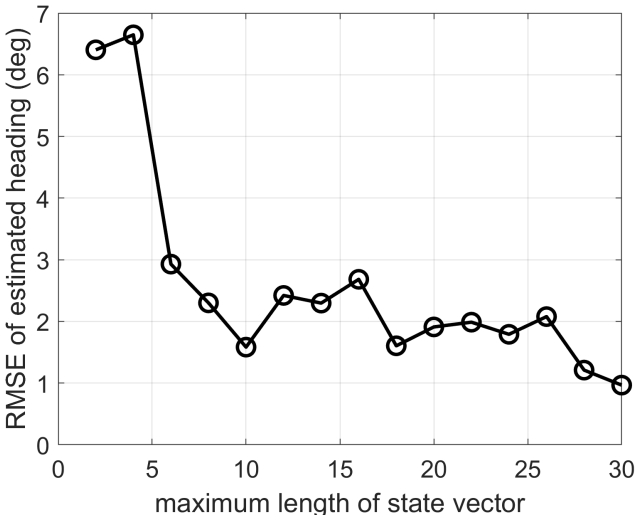

Fig. 3. RMSE of estimated heading with different state vector length.

heading estimation. The slowly changing error is also caused by the accumulation of linearization error of measurement model used in EKF. Instead, the proposed algorithm can obtain a stable heading estimation during the whole trajectory.

To calculate the Root Mean Square Errors (RMSEs) of estimated heading angle with different maximum length of error state vector, another experiment was designed and the results are shown in Fig. 3. The RMSE is calculated during a straight part of a playground track with a duration of 20 seconds walking, while the estimates in the circular parts are ignored since the ground truth is hard to match. In the experiment, the actor's arm keeps static with body to avoid the error caused by arm swing, and the deviation between the ending sensor heading and the starting sensor heading is used to evaluate our algorithm. As shown in the figure, RMSE decreases when using more states in the error state vector. There is a large drop on RMSE when the maximum length of error state vector grows from 2 to 10. It shows the benefit from multiple observations used in the multi-state constrained filter.

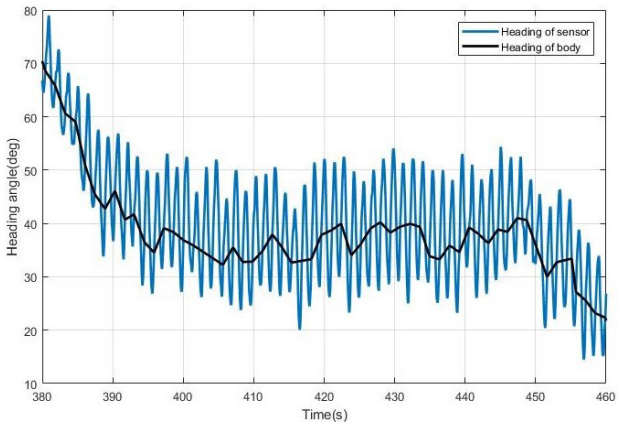

Fig. 4. PDR trajectories with different states number.

The performance of the proposed algorithm improves slowly if the maximum length keeps increasing from 10. When 30 states are used in the proposed filter, which means the update interval of attitude estimation is about 15 seconds, the RMSE of estimated heading angle is less than 1 degree.

We designed a classic pedestrian dead-reckon (PDR) experiment [19] to further evaluate the influence of state vector length on estimation performance. The actor keeps a uniform swing arm posture and forward speed, walked on the playground for about 2 loops, the trajectory coincides with the runway line, and the start point coincides with the end point. The trajectory of walking is used for evaluating the performance of the proposed algorithm. The trajectory is obtained as follows,

$$\begin{cases} x_n = x_{n-1} + L_n \cos\theta_n \\ y_n = y_{n-1} + L_n \sin\theta_n \end{cases} \tag{28}$$

where (x_n, y_n) is the coordinates after the n-th pace in the horizontal plane, θ_n is the estimated heading angle, and L_n is the pace length. L_n is calculate by GNSS trajectory as (29),

$$L_n = \sqrt{(x_{GNSS,n} - x_{GNSS,n-1})^2 + (y_{GNSS,n} - y_{GNSS,n-1})^2} \tag{29}$$

where $(x_{GNSS,n}, y_{GNSS,n})$ is the GNSS coordinates after the n-th step in the horizontal plane. In addition, it is assumed that the moment when the angular velocity is maximum is the moment when the heading of the human body and the sensor are consistent in each swing arm cycle. The peak time of gyroscope raw data is used as the step time of each step of the actor to ensure that the heading angle of the handheld smart phone is consistent with the human body at the selected step time in each swing arm cycle. Before selecting the pace time, uses 30-order smoothing filter to remove the pseudo-peak of gyroscope data. The selection result of body heading is shown in Fig. 4.

Under the uniform swing arm movement, the selection method will bring a fixed error between the selected body heading and the real body heading. Based on the previous experiment, assuming that the estimation error of our algorithm can be ignored within 10 seconds, we rotated the first

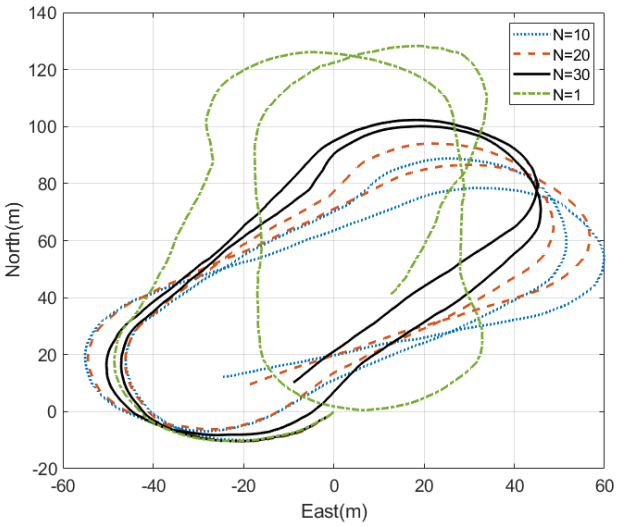

Fig. 5. PDR trajectories with different states number.

TABLE II
END POINT ERROR OF PDR TRAJECTORIES WITH DIFFERENT STATES NUMBER

	Maximum length of error state vector (N)			
	1(EKF)	10	20	30
End Point Error (Meter)	43.13	27.50	21.47	13.63
Relative Accuracy	5.39%	3.44%	2.68%	1.70%

10 seconds trajectory and heading of each experiment to match the GNSS trajectory to correct this fixed error.

The PDR results are shown in Fig. 5, where the maximum length of error state vector $N = 10, 20, 30$ are chosen for comparison. The trajectory obtained from EKF is also compared in the figure, which is denoted by $N = 1$. It is obvious that the trajectory obtained from EKF is distorted heavily from the ground truth. The proposed algorithm can provide stable estimates of heading angles during the trajectory. The error of the estimated heading angles can be reduced by increasing the maximum length of error state vector, which can furtherly reduce the positioning error of the PDR trajectory.

The ground truth of the start point and end point of the trajectory is the same, so the end point error can be obtained for performance evaluation, as shown in Table II. The end point error is decreasing as the maximum length of error state vector is growing. When 30 states are used in the proposed algorithm, the proposed algorithm can provide an end point error of 13.63m during the whole 800 meter-length trajectory, and the relative positioning accuracy is 1.70% of the total trajectory length.

To analyze the impact of geomagnetic interference caused by buildings or metal objects around such as cars or street lamps, the performance of the proposed algorithm is also

Fig. 6. City road scenario for performance evaluation.

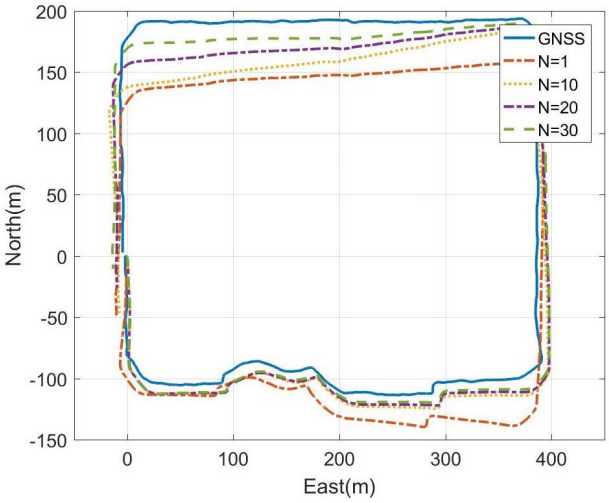

Fig. 7. PDR trajectories with different states number in city road scenario.

evaluated in a city road scenario, as shown in Fig. 6. A typical city road scenario around a city square is chosen, and different types of vehicles are parked along the road. The total length of the trajectory is about 1.4 km, and the walking duration is nearly 15 minutes. In the process of moving, our actor also keep a uniform swing arm posture and forward speed, the trajectory calculation method is the same as the above experiment in equation (28) and (29). Different maximum error state vector lengths are used for comparison, and the positioning results obtained from GNSS are used as the ground truth to evaluate the positioning accuracy of the proposed algorithm.

The results are shown in Fig. 7, also choose the maximum length of state vector $N = 10, 20, 30$. The proposed algorithm can provide stable estimates of heading angles during the city road scenario, the heading angle estimation error could reduce with the increase of the maximum length of error state vector.

As shown in the approximate square trajectory in Fig. 7, Huge trajectory error mainly occurs after the first turning (The coordinates are approximately (100,−100) to (400,−100)) and the third turning (The coordinates are approximately (400,200) to (0,200)). Among the four trajectories, the trajectory error of $N = 1$ is the largest, and the trajectory error will decrease with the increase of N. In our experiment, when N is increased to 30, the positioning performance is better than other state vector lengths.

These huge trajectory errors are caused by the distortion of geomagnetic field, because heading estimation should diverge slowly and evenly when the geomagnetic observation is not

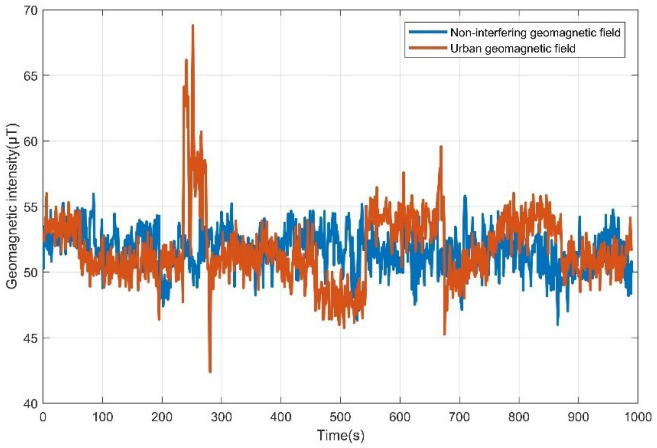

Fig. 8. Geomagnetic distortion in city road scenario.

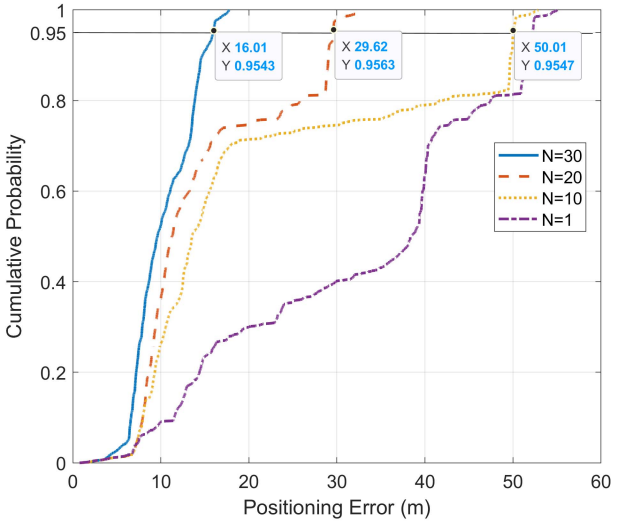

Fig. 9. CDF statistics with different states number in city road scenario.

interfered. We calculated the geomagnetic intensity in the urban environment experiments, and intercepted a group of data with the same length from the undisturbed geomagnetic data measured in the playground previously, to explain the geomagnetic status of the urban experiment. The comparison results are shown in Fig. 8.

As shown in Fig. 8, At 200 to 300 seconds and about 450 to 850 seconds, the estimation of geomagnetic field is distorted. In 200 to 300 seconds (after the first turning), metal objects are sparsely distributed in the street, the distortion amplitude of geomagnetic observation is small, and the duration is short, during this period, the trajectories difference estimated by different maximum lengths of state vectors are small. In about 450 to 850 seconds (after the third turning), the distribution of metal objects (parked cars) along the street becomes dense, the duration of distortion becomes longer, the positioning error increases rapidly after passing through the third turning, during this period, it shows better heading angle estimation performance with longer maximum length of error state vector. The specific cumulative error statistical analysis is shown in Fig. 9, and the comparison with EKF algorithm is added.

The original GNSS positioning data sampling frequency is 1Hz, the GNSS positioning data in each pace time is

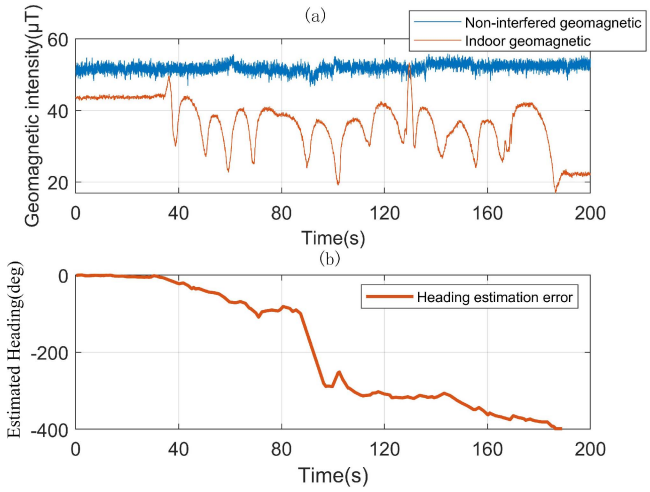

Fig. 10. Indoor experiment (a) indoor geomagnetic field,(b) estimated heading.

used as the reference for accumulative error statistics after interpolating it to 50hz (magnetometer sampling frequency). Fig. 9 is a CDF curve of positioning error for error state vectors with 4 different maximum lengths (N = 30, 20, 10, 1), at a probability of 95%, when 30 states are used in the proposed algorithm, the proposed algorithm can provide cumulative error of 16.01m, when 10 states are used in proposed algorithm, it can provide cumulative error of 50.01m, it is close to EKF algorithm.

An indoor experiment is added to evaluate the performance of the proposed algorithm. The indoor environment is a typical office building, which contains a long corridor with similar rooms on each side. The actor walked strictly along a straight line calibrated in advance on the ground. Therefore, the ground-truth of the heading angle should be a constant. The intensity of indoor geomagnetic field sampled along the trajectory is shown in Fig. 10(a). We can find heavy distortion in the indoor geomagnetic field, which may be induced by the steel skeleton of the building. The estimated heading of walking is shown in Fig 10(b). As we can see, the heading error exceeded 350 degrees during the trajectory, and there are many mutations in the curve, it is completely different from the real walking situation. Due to the huge and rapid changing distortion in the indoor geomagnetic field, the proposed algorithm fails to converge.

V. Conclusion

In this paper, a new heading angle estimation method based on multi-state constrained Kalman filter with low-cost sensor is proposed. The estimation is realized by sequential observation of geomagnetic field. Compared with other related work, the method proposed in this paper eliminates the dependence on gravity direction, avoids the strong noise effect caused by the additional linear acceleration in the motion state, and reduces the effect of insufficient observation when using magnetic field observation alone, finally, realizes the sensitive tracking of the heading angle during walking with uniform swing arm posture and forward speed. The experiments in ideal runway scenario and typical city road scenario are carried

out to evaluate the performance and anti-interference ability of the algorithm. In the application scenario of wearable devices during movement, the algorithm proposed in this paper can provide stable real-time heading angle tracking under low-cost sensors, and the estimation accuracy will increase with the increase of the maximum length of state vector. However, the proposed algorithm cannot be used in indoor scenarios where the geomagnetic filed is heavily distorted.

ACKNOWLEDGMENT

The authors gratefully acknowledge the assistance of Fengyi Zhou for designing the graphic abstract.

REFERENCES

[1] B. Barshan and H. F. Durrant-Whyte, "Inertial navigation systems for mobile robots," *IEEE Trans. Robot. Autom.*, vol. 11, no. 3, pp. 328–342, Jun. 1995.
[2] L. Ojeda and J. Borenstein, "FLEXnav: Fuzzy logic expert rule-based position estimation for mobile robots on rugged terrain," in *Proc. IEEE Int. Conf. Robot. Automat.*, vol. 1, May 2002, pp. 317–322.
[3] S. K. Hong, "Fuzzy logic based closed-loop strapdown attitude system for unmanned aerial vehicle (UAV)," *Sens. Actuators A, Phys.*, vol. 107, no. 2, pp. 109–118, Oct. 2003.
[4] S. Beauregard, "Omnidirectional pedestrian navigation for first responders," in *Proc. 4th Workshop Positioning, Navigat. Commun.*, Mar. 2007, pp. 33–36.
[5] D. Titterton, J. L. Weston, and J. Weston, *Strapdown Inertial Navigation Technology*, vol. 17. Edison, NJ, USA: IET, 2004.
[6] H. J. Luinge and P. H. Veltink, "Inclination measurement of human movement using a 3-D accelerometer with autocalibration," *IEEE Trans. Neural Syst. Rehabil. Eng.*, vol. 12, no. 1, pp. 112–121, Mar. 2004.
[7] H. Zhou and H. Hu, "Human motion tracking for rehabilitation—A survey," *Biomed. Signal Process. Control*, vol. 3, no. 1, pp. 1–18, Jan. 2008.
[8] S. O. H. Madgwick, A. J. L. Harrison, and R. Vaidyanathan, "Estimation of IMU and MARG orientation using a gradient descent algorithm," in *Proc. IEEE Int. Conf. Rehabil. Robot.*, Jun. 2011, pp. 1–7.
[9] L. Wohle and M. Gebhard, "A robust quaternion based Kalman filter using a gradient descent algorithm for orientation measurement," in *Proc. IEEE Int. Instrum. Meas. Technol. Conf. (IMTC)*, May 2018, pp. 1–6.
[10] M. Admiraal, S. Wilson, and R. Vaidyanathan, "Improved formulation of the IMU and MARG orientation gradient descent algorithm for motion tracking in human-machine interfaces," in *Proc. IEEE Int. Conf. Multisensor Fusion Integr. Intell. Syst. (MFI)*, Nov. 2017, pp. 403–410.
[11] S. Habbachi, M. Sayadi, and N. Rezzoug, "Partical filtering for orientation determining using inertial sensors IMU," in *Proc. 4th Int. Conf. Adv. Technol. Signal Image Process. (ATSIP)*, Mar. 2018, pp. 1–5.
[12] A. M. Sabatini, "Kalman-filter-based orientation determination using inertial/magnetic sensors: Observability analysis and performance evaluation," *Sensors*, vol. 11, no. 10, pp. 9182–9206, 2011.
[13] S. Zihajehzadeh, D. Loh, M. Lee, R. Hoskinson, and E. J. Park, "A cascaded two-step Kalman filter for estimation of human body segment orientation using MEMS-IMU," in *Proc. 36th Annu. Int. Conf. IEEE Eng. Med. Biol. Soc.*, Aug. 2014, pp. 6270–6273.
[14] D. Q. Duong, J. Sun, T. P. Nguyen, and L. Luo, "Attitude estimation by using MEMS IMU with fuzzy tuned complementary filter," in *Proc. IEEE Int. Conf. Electron. Inf. Commun. Technol. (ICEICT)*, Aug. 2016, pp. 372–378.
[15] H. Ahmed and M. Tahir, "Improving the accuracy of human body orientation estimation with wearable IMU sensors," *IEEE Trans. Instrum. Meas.*, vol. 66, no. 3, pp. 535–542, Mar. 2017.
[16] Y. Wu, D. Zou, P. Liu, and W. Yu, "Dynamic magnetometer calibration and alignment to inertial sensors by Kalman filtering," *IEEE Trans. Control Syst. Technol.*, vol. 26, no. 2, pp. 716–723, Mar. 2018.
[17] A. I. Mourikis and S. I. Roumeliotis, "A multi-state constraint Kalman filter for vision-aided inertial navigation," in *Proc. IEEE Int. Conf. Robot. Automat.*, Apr. 2007, pp. 3565–3572.
[18] T. Tan, A. Peng, J. Huang, L. Zheng, and G. Ou, "A gyroscope bias estimation algorithm based on map specific information," *Sensors*, vol. 18, no. 8, p. 2534, Aug. 2018.
[19] L. Zheng, W. Zhou, W. Tang, X. Zheng, A. Peng, and H. Zheng, "A 3D indoor positioning system based on low-cost MEMS sensors," *Simul. Model. Pract. Theory*, vol. 65, pp. 45–56, Jun. 2016.

Ye Tian received the M.Sc. degree in communication and information systems from Xiamen University in 2020. He is a newly graduated master and has completed his research as a member of Dr. Ao Peng's Laboratory. His research contents include integrated navigation and GNSS anti-spoofing technology. He will soon start his doctoral work in an application field in location-based service (LBS).

Ao Peng (Member, IEEE) received the M.Sc. and Ph.D. degrees in communication and information systems from Xiamen University, Fujian, China, in 2011 and 2014, respectively. In 2015, he joined the School of Informatics, Xiamen University, where he is currently an Assistant Professor. His research interests include satellite navigation, indoor navigation, and multi-source positioning and navigation.

Xueting Xu (Student Member, IEEE) received the B.S. degree from Nanjing University of Science and Technology, Nanjing, China. She is currently pursuing the Ph.D. degree in communication and information systems with Xiamen University, China. Her research interests include wireless communications, 5G positioning, and all-source poisitioning and navigation (ASPN).

Weicheng Zhang (Graduate Student Member, IEEE) received the B.S. degree in communication and information systems from Xiamen University in 2019, where he is currently pursuing the master's degree in communication engineering. He is doing research as a member of Dr. Xueming Hong's Laboratory. His research contents include 5G communication systems, machine semantics, and deep learning.